

# Separating True V0's from Combinatoric Background with a Neural Network

Marvin Justice<sup>1</sup>

*Department of Physics and Center for Nuclear Research, Kent State University,  
Kent, OH 44242*

---

## Abstract

A feedforward multilayered neural network has been trained to “recognize” true V0's in the presence of a large combinatoric background using simulated data for 2 GeV/nucleon Ni + Cu interactions. The resulting neural network filter has been applied to actual data from the EOS TPC experiment. An enhancement of signal to background over more traditional selection mechanisms has been observed.

---

## 1 Introduction

A high statistics sample of  $\Lambda$ 's and  $K_s^0$ 's produced in 2 GeV/nucleon Ni + Cu collisions has been obtained with the EOS Time Projection Chamber [1]. These neutral strange particles, or V0's, are reconstructed through their charged particle decays:  $\Lambda \rightarrow p + \pi^-$  and  $K_s^0 \rightarrow \pi^+ + \pi^-$ . The acceptance plus efficiency for detecting true V0's with the EOS TPC is very good; however, the sample is contaminated by a large combinatoric background of false  $\Lambda$ 's and  $K_s^0$ 's (*e.g.*  $\sim 40,000 p\pi^-$  pairs for every true  $\Lambda$ ).

Traditionally, the signal is extracted from the background by cutting on certain parameters — such as distance of decay from the main vertex — whose distributions are different for signal and background. Inevitably, such cuts eliminate a significant fraction of the signal as well and one is confronted with the task of how to optimize the cuts. The optimization problem is a natural candidate for neural network techniques. A feedforward, multilayered neural network filter has been devised which, when applied to the EOS data, results in a cleaner, higher statistics sample of  $\Lambda$ 's and  $K_s^0$ 's.

---

<sup>1</sup> Tel. +1 510 486 6531, e-mail justice@sseos.lbl.gov

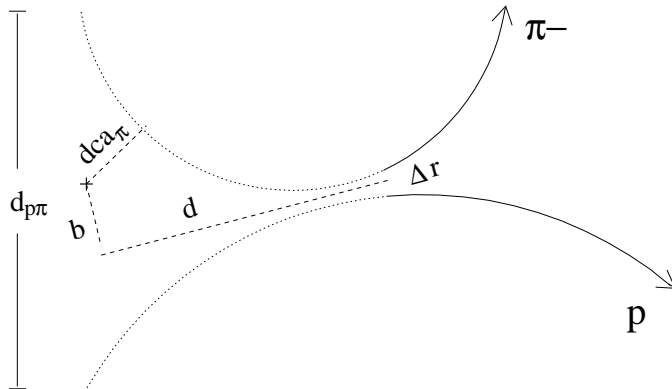


Fig. 1. Schematic diagram illustrating  $\Lambda$  decay and reconstruction.

## 2 V0 Reconstruction

A schematic diagram illustrating  $\Lambda$  reconstruction and the set of parameters used to separate the signal from the background is shown in Fig. 1. V0 reconstruction begins after all TPC tracks in an event have been found and the overall event vertex has been determined. In the case of  $\Lambda$ 's, each pair of  $p\pi^-$  tracks is looped over and their point of closest approach is calculated. Pairs whose trajectories approximately intersect at a point other than the main vertex are fit with a V0 hypothesis from which the invariant mass, momentum, and point of decay ( $\vec{X}_\Lambda$ ) are extracted.

The  $\Lambda$  momentum vector is projected back to the target to obtain  $d$ , the distance between  $\vec{X}_\Lambda$  and the overall event vertex, and  $b$ , the impact parameter or distance of closest approach between the event vertex and the  $\Lambda$  trajectory. Likewise, the proton and  $\pi^-$  tracks are projected back to the target to obtain  $dca_p$  and  $dca_\pi$  which are the distances of closest approach of the daughter particle trajectories to the main vertex. Another useful variable, closely related to the two  $dca$ 's, is the distance between the  $p$  and  $\pi^-$  trajectories at the target plane,  $d_{p\pi}$ ; while the distance between the  $p$  and  $\pi^-$  trajectories at  $\vec{X}_\Lambda$  is called  $\Delta r$ . In an ideal detector  $b$  and  $\Delta r$  would be exactly zero for true  $\Lambda$ 's and  $K_s^0$ 's. In any real detector, of course, these quantities will take on finite values. The estimated impact parameter resolution for the EOS TPC is  $\sigma_b \sim 3$  mm.

Seven parameters are cut on to separate true  $\Lambda$ 's and  $K_s^0$ 's from the background:  $d$ ,  $b$ ,  $\Delta r$ ,  $d_{p\pi}$ ,  $dca_p$ ,  $dca_\pi$ , and the  $\chi^2/\nu$  of the combined fit to the V0 hypothesis. The traditional method is to simply define a seven dimensional cut such as:  $d \geq 4$  cm AND  $b \leq 3$  mm AND  $d_{p\pi} \geq 2$  cm AND etc. The

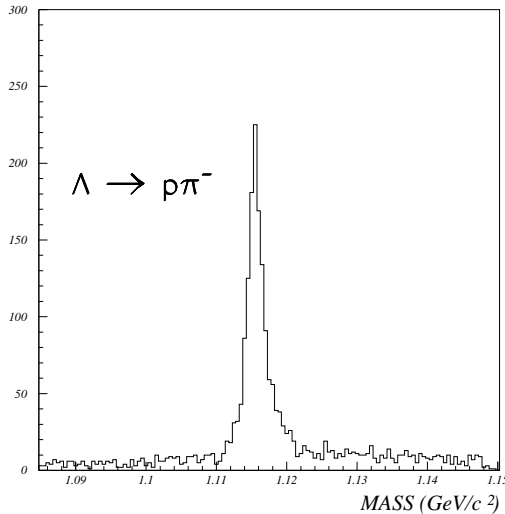


Fig. 2.  $\Lambda$  invariant mass spectrum from seven parameter cuts.

problem then becomes what the precise values of the cuts should be. For example, nearly all of the combinatoric background can be eliminated by simply requiring that  $d$  be very large. Since the true  $V0$ 's follow an exponential decay law, however, such a cut would throw out most of the true signal as well.

For the EOS data, an attempt to optimize the cuts has been made through trial and error using the invariant mass distribution as a guide. The invariant mass distribution resulting from the “best” cuts for  $\Lambda$ 's is shown in Fig. 2. From Monte Carlo simulations it is estimated that over 60% of the reconstructed true  $\Lambda$ 's are lost in making the cuts necessary to obtain the background level in this plot.

Clearly, searching a seven dimensional parameter space by trial and error in an effort to optimize the cuts can be a very tedious process. In addition, the high degree of correlation among some of the parameters makes it unlikely that the optimum cut would be obtained by cutting perpendicular to each of the seven axes as above. An uncorrelated set of parameters could be formed from linear combinations of the original seven parameters by using a principal component analysis. However, one would still be left with the task of optimizing the cuts in the new parameter space. Moreover, any boundary surface chosen to separate the true  $V0$ 's from the background would still be restricted to a seven dimensional polyhedron. An alternative method of cutting, which may allow for more complicated shapes in the seven dimensional space, is provided by neural network techniques.

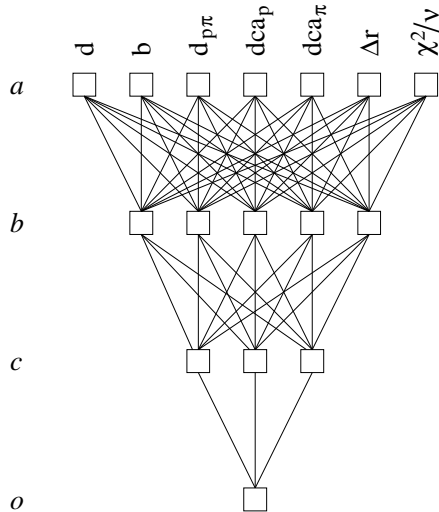


Fig. 3. V0 neural network topology.

### 3 Neural Network Approach

A general feedforward multilayered network consists of a set of input neurons, one or more layers of hidden neurons, a set of output neurons, and synapses connecting each layer to the subsequent layer [2]. A particular network topology for the application at hand is shown in Fig. 3 where the inputs,  $a_i$ , are the seven V0 parameters. There are two hidden layers,  $b_j$  and  $c_k$ , and one output,  $o$ . The network is fully connected in the sense that there is a synapse connecting each  $a$  neuron to each  $b$  neuron, each  $b$  neuron to each  $c$  neuron, and each  $c$  neuron to the output. Given a set of inputs, the rules for calculating  $o$  are:

$$b_j = \tanh \left( \sum_i w_{ij}^{ab} a_i - \Theta_j \right), \quad (1)$$

$$c_k = \tanh \left( \sum_j w_{jk}^{bc} b_j - \Theta_k \right), \quad (2)$$

$$o = \sum_k w_k^{co} c_k, \quad (3)$$

where the  $w$ 's are synaptic weights and the  $\Theta$ 's are thresholds.

For the current application one would like  $o$  to take on one value for true V0's and a different value for false V0's, *e.g.* +1 for true and -1 for false. The problem then becomes one of finding a set of weights and thresholds that give the desired outputs. In general, this is accomplished by starting with random initial guesses for the  $w$ 's and  $\Theta$ 's and "teaching" the network with a training set and a backpropagation algorithm.

A set of  $\sim 2.5 \times 10^5$  2 GeV/nucleon Ni + Cu events generated with the ARC cascade code [3] has been used to train and test the network of Fig. 3. Only those events which had some strangeness content in the final state were used in the training stage. The strange events were run through a detailed GEANT simulation of the TPC and passed through the same analysis chain as was the real data. Loose cuts on the seven V0 parameters were applied to the output in order to weed out easy background. The resulting training set was composed of 3757 true V0's and 41,600 combinatoric V0's. The V0's were labeled as being either true or false based on information stored from GEANT and were then passed one at a time through the neural net. Separate, though topologically identical, networks were used for  $\Lambda$ 's and  $K_s^0$ 's.

As each V0 is passed through its appropriate network the weights and thresholds are adjusted so that the actual output approaches the desired output. This is done by minimizing the error function:

$$\begin{aligned}
 E &= \frac{1}{2}(t - o)^2 \\
 &= \frac{1}{2}\left(t - \sum_k w_k^{co} c_k\right)^2,
 \end{aligned}
 \tag{4}$$

where  $t = +1$  for true V0's and  $t = -1$  for background or fake V0's. A simple gradient descent algorithm:

$$\Delta w_{ij}^{\alpha\beta} = -\eta \frac{\partial E}{\partial w_{ij}^{\alpha\beta}},
 \tag{5}$$

$$\Delta \Theta_i = -\eta \frac{\partial E}{\partial \Theta_i},
 \tag{6}$$

is used to adjust the  $w$ 's and  $\Theta$ 's after  $o$  is calculated for each V0. In the present application  $\eta$  was chosen to be 0.05 and all of the thresholds were held fixed at zero.

In principle, the training process should continue until the weights cease to change. In practice the same set of events was passed repeatedly through the network in alternating training and testing cycles. After each training cycle the events were filtered back through the network and a histogram of the resulting outputs (similar to Fig. 4) was visually inspected to judge convergence. The cpu time per training cycle was  $\sim 12$  minutes on a 55 MHz HyperSparc. After 10 cycles the networks were judged to have converged.

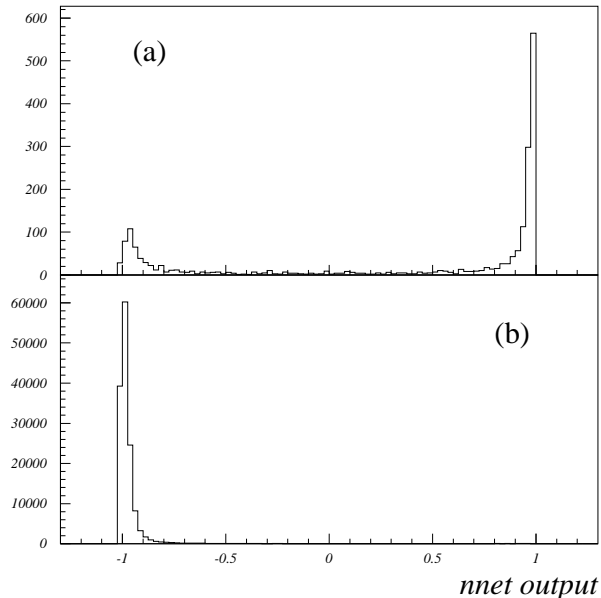


Fig. 4. Neural network output for (a) true and (b) false Monte Carlo  $\Lambda$ 's.

## 4 Results

The performance of the networks was first tested on a subset of  $\sim 1.73 \times 10^5$  ARC events which had not been preselected for strangeness. Although all of the events containing  $V0$ 's in this subset were also members of the training set, they had been rerun through GEANT with different random number seeds. The same loose cuts on the seven parameters were applied to the GEANT output as in the training phase resulting in 2601 true and  $\sim 1.75 \times 10^5$  false  $V0$ 's — roughly the same 1:7 ratio as is observed in the EOS data after loose cuts. The  $V0$ 's were passed through the neural network filters and the resulting distributions of outputs for  $\Lambda$ 's are shown in Fig. 4.

Qualitatively, one sees that the  $\Lambda$  network performs as desired: the distribution for the true's has a sharp peak at +1 while the combinatoric distribution is peaked at -1. Quantitatively, one can define a purity:

$$Purity = \frac{true}{true + false} ,$$

and a yield:

$$Yield = \frac{detected\ true}{actual\ true} .$$

The purity and yield factors for the traditional method of cutting and for cuts

cut method	Purity (%)	Yield (%)
traditional	93.7	15.6
$nnet \geq 0.50$	91.5	23.2
$nnet \geq 0.60$	92.8	22.6
$nnet \geq 0.70$	93.6	22.1
$nnet \geq 0.80$	95.4	21.1
$nnet \geq 0.90$	97.2	19.2
$nnet \geq 0.95$	99.0	16.2

Table 1: Purity and yield factors for Monte Carlo  $\Lambda$ 's.

on the value of the neural network output are listed in Table 1. All yields reflect a common  $\sim 60\%$  loss factor arising from geometrical acceptance and tracking efficiency. From the table one sees that, for the Monte Carlo events, the neural network method gives a significantly higher yield than the traditional method at the same level of purity. Alternatively, higher purity levels can be obtained without loss of yield. Similar results are obtained with the  $K_s^0$  network.

The ultimate test of a neural network filter is its performance on actual data. Although yield and purity factors cannot be calculated, the overall performance can be judged by comparing the invariant mass distributions which results from cutting on  $o$  to those which result from the traditional method of cutting. The distribution for EOS  $\Lambda$ 's obtained by requiring  $o \geq 0.95$  is shown in Fig. 5 on the same scale as the distribution of Fig. 2. A higher peak and lower background are clearly evident in the neural net filtered distribution. When invariant mass cuts are applied ( $1112 \text{ MeV}/c^2 \leq M_\Lambda \leq 1120 \text{ MeV}/c^2$ ), the neural net method gives 1797  $\Lambda$  candidates as opposed to 1362 for the traditional method.

## 5 Conclusions

For the EOS TPC data the neural network approach results in significant enhancements in both the yields and purities of  $\Lambda$ 's and  $K_s^0$ 's compared to the straightforward method of cutting in seven dimensional parameter space. The  $\Lambda$  candidates in the peaks of Figs. 2 and 5 were projected onto the seven parameter axes and a comparison of the resulting distributions was made. In general, the edges of the neural network filtered events are less sharp; lending support to the intuitive notion that the neural filter finds a smoother hypersurface in the parameter space.

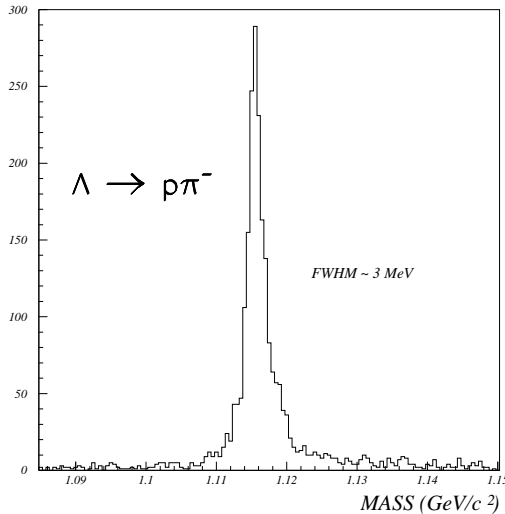


Fig. 5.  $\Lambda$  invariant mass spectrum from neural network cut.

When working with neural network filters it is obviously important to insure that the training set matches the data to be filtered as closely as possible. This was observed in the present study when the neural network was initially trained with a set of ARC events which did not include the coalescence of protons and neutrons to form deuterons. The result were V0 neural networks which performed only marginally better than the seven parameter cuts method.

The neural network topology of Fig. 3 was found to work so well that other topologies were not investigated. It is possible that alternative network architectures could give even better results. One of the disadvantages of the neural network approach is that there exists no *a priori* prescription for evaluating various topologies — one must simply proceed through trial and error.

The cpu time spent in training the networks was not significant; however, the time spent in generating the training set was quite large:  $\sim 5$  cpu minutes/event  $\times \sim 17,000$  strange ARC events. Since the GEANT simulations were being done anyway in order to study acceptance and efficiency issues the net cpu overhead on data processing due to neural network training can be considered to be negligible.

## Acknowledgements

The author would like to thank David Kahana for providing the ARC events. This work is supported in part by the US Department of Energy under contracts/grants DE-AC03-76SF00098, DE-FG02-89ER40531, DE-FG02-88ER40408,

DE-FG02-88ER40412, DE-FG05-88ER40437, and by the US National Science Foundation under grant PHY-9123301.

## References

- [1] M. Justice, S. Albergo, F. Bieser, F.P. Brady, Z. Caccia, D. Cebra, A.D. Chacon, J. Chance, Y. Choi, S. Costa, J. Elliott, M. Gilkes, J. Hauger, A. Hirsch, E. Hjort, A. Insolia, D. Keane, J. Kintner, M. Lisa, H. Matis, R. McGrath, M. McMahan, C. McParland, D. Olson, M. Partlan, N. Porile, R. Potenza, G. Rai, J. Rasmussen, H.G. Ritter, J. Romanski, J. Romero, G. Russo, R. Scharenberg, A. Scott, Y. Shao, B. Srivastava, T.J.M. Symons, M. Tincknell, C. Tuvé, S. Wang, P. Warren, D. Weerasundara, H. Wieman, and K. Wolf; Proc. of Quark Matter '95, Nucl. Phys. **A590**, 549c (1995).
- [2] See, for example: B.Müller and J.Reinhardt, *Neural Networks An Introduction*, (Springer Verlag, Berlin, 1991).
- [3] Y. Pang, T.J. Schlagel, and S.H. Kahana, Phys. Rev. Lett. **68**, 2743 (1992).